COLD SPRING HARBOR
Molecular Case Studies

RESEARCH REPORT

Double paternal uniparental isodisomy 7 and 15 presenting with Beckwith–Wiedemann spectrum features

Siren Berland,[1] Cecilie F. Rustad,[2] Mariann H. L. Bentsen,[3] Embjørg J. Wollen,[4] Gitta Turowski,[5] Stefan Johansson,[1,6] Gunnar Houge,[1] and Bjørn I. Haukanes[1]

[1]Department of Medical Genetics, Haukeland University Hospital, 5021 Bergen, Norway; [2]Department of Medical Genetics, Oslo University Hospital, 0424 Oslo, Norway; [3]Department of Pediatric and Adolescent Medicine, Haukeland University Hospital, 5021 Bergen, Norway; [4]Department of Pediatric Hepatology, Division of Pediatric and Adolescent Medicine, University of Oslo, Oslo University Hospital HF, 0424 Oslo, Norway; [5]Department of Pathology, Center for Perinatal and Pregnancy-Related Pathology, Oslo University Hospital-Ullevål, 0424 Oslo, Norway; [6]Department of Clinical Science, University of Bergen, 5007 Bergen, Norway

Abstract Here we describe for the first time double paternal uniparental isodisomy (iUPD) 7 and 15 in a baby boy with features in the Beckwith–Wiedemann syndrome spectrum (BWSp) (placentomegaly, hyperinsulinism, enlarged viscera, hemangiomas, and earlobe creases) in addition to conjugated hyperbilirubinemia. His phenotype was also reminiscent of genome-wide paternal uniparental isodisomy. We discuss the most likely origin of the UPDs: a maternal double monosomy 7 and 15 rescued by duplication of the paternal chromosomes after fertilization. So far, paternal UPD7 is not associated with an abnormal phenotype, whereas paternal UPD15 causes Angelman syndrome. Methylation analysis for other clinically relevant imprinting disorders, including BWSp, was normal. Therefore, we hypothesized that the double UPD affected other imprinted genes. To look for such effects, patient fibroblast RNA was isolated and analyzed for differential expression compared to six controls. We did not find apparent transcription differences in imprinted genes outside Chromosomes 7 and 15 in patient fibroblast. *PEG10* (7q21.3) was the only paternally imprinted gene on these chromosomes up-regulated beyond double-dose expectation (six-fold). We speculate that a high *PEG10* level could have a growth-promoting effect as his phenotype was not related to aberrations in BWS locus on 11p15.5 after DNA, RNA, and methylation testing. However, many genes in gene sets associated with growth were up-regulated. This case broadens the phenotypic spectrum of UPDs but does not show evidence of involvement of an imprinted gene network.

[Supplemental material is available for this article.]

Corresponding author:
siren.berland@helse-bergen.no

Ontology terms: conjugated hyperbilirubinemia; hyperinsulinemic hypoglycemia; large placenta; overgrowth

Published by Cold Spring Harbor Laboratory Press

doi:10.1101/mcs.a006113

INTRODUCTION

In uniparental disomy (UPD), both chromosomes in a pair are derived from the same parent (Engel 1980). The two chromosomes can be identical (isodisomy) or homologous (heterodisomy). Meiotic or mitotic recombination can result in a mixture of homozygous (identical) and heterozygous segments. Most UPDs are of maternal origin and caused by trisomy rescue after errors in the first meiotic cleavage (MI) in the oocyte (Kotzot and Utermann 2005; Nakka et al. 2019). In contrast, complete isodisomies are often of paternal origin (Scuffins et al. 2021). Gamete complementation is an anecdotal cause of UPD (Liehr 2014). Segmental UPDs due to mitotic recombination of the maternal and paternal homologs often display mosaicism.

UPDs can be phenotypically neutral but can also be associated with disease in multiple ways; imprinting disorder, low-level mosaicism of an original aneuploidy, a more complex event (supernumerary marker chromosomes, chromothripsis), or demasking of a recessive disease caused by a pathogenic variant carried by only one of the parents. Imprinted genes are tightly regulated, resulting in monoallelic expression in a parent-of-origin-specific and sometimes tissue-dependent manner. Chromosomes 6, 7, 11, 14, 15, and 20 contain imprinted genes that can result in abnormal development if the chromosome pair derives from one parent only. Remarkably, developmental disorders related to imprinting often have overlapping features. Growth disturbances are common, and paternal UPDs often lead to increased intrauterine growth (paternal UPD6/11/14/20 and mosaic genome-wide paternal UPD), whereas many maternal UPDs cause growth restrictions (maternal UPD7/11/14/15/20 and mosaic genome-wide maternal UPD). Endocrine dysregulation and neurodevelopmental delay are also frequently observed in imprinting disorders.

Complete (nonsegmental) UPDs are rare in the general population but show a higher incidence in patient populations. UPD was found in 3.73% of discarded morphologically abnormal embryos (Xu et al. 2015) and in 0.31% of about 32,000 diagnostic exome trios, of which 39% were isodisomies (Scuffins et al. 2021). No double UPD was found in this large patient study. A population screen suggested that UPD occurs in 1/2000 births (0.05%) (Nakka et al. 2019). This study also reported six double UPDs without further details, and their data suggested an incidence of double UPD of 1/50,000 births. The most frequent UPDs in this data set involved Chromosomes 1, 4, 16, 21, 22, and X. This contrasts with the UPDs found after literature search in patient populations, in which all involved imprinted chromosomes (Chromosomes 6, 7, 11, 14, and 15). The mothers of children with UPDs were significantly older than those of non-UPD children, implying a maternal age effect due to meiotic errors (Nakka et al. 2019; Scuffins et al. 2021).

Chromosome 15 is the most common chromosome involved in UPD formations in diagnostic settings, accounting for both maternal and paternal UPDs (Scuffins et al. 2021). Previous publications describing UPDs found a general overrepresentation of imprinted chromosomes like Chromosome 7 (Liehr 2014), but this probably reflects an ascertainment bias as these present with a recognizable phenotype and have readily available diagnostic tests in most developed countries (Nakka et al. 2019). UPD(15)mat (maternal UPD15) often displays heterodisomy (hUPD) or mixed hUPD and isodisomy (iUPD) and result from trisomy rescue. UPD(15)mat is found in ~25% of Prader–Willi syndrome (PWS) patients (Grugni et al. 2008), whereas UPD(15)pat (often iUPD) is a rare cause of Angelman syndrome, present in ~6% (den Besten et al. 2021). iUPD(15)pat can be caused by postzygotic monosomy 15 rescue after maternal meiotic errors, mitotic segregation errors, or rescue of an isochromosome formation. In contrast, paternal hUPD due to trisomy rescue after a paternal meiotic error is rare (Engel 2006). Angelman syndrome is caused by the lack of the maternally expressed UBE3A in the brain. The phenotype includes mild neonatal hypotonia, epilepsy, a characteristic face, microcephaly, ataxia, usually severe developmental delay without expressed language, and a normal life span, but no overgrowth (den Besten et al. 2021).

UPD(7)mat is a cause of Silver–Russell syndrome (SRS), a growth-restricted syndrome. UPD(7)pat is regarded as phenotypically neutral unless a recessive disease is demasked (Hoffmann and Heller 2011), although one report on tall stature suggested a contrasting growth effect (Nakamura et al. 2018). In total, there are seven previous clinical reports on UPD(7)pat patients, five of whom had *CFTR*-related disease (Fares et al. 2006; Feuk et al. 2006; Goh et al. 2007; Le Caignec et al. 2007), including one patient with both cystic fibrosis (CF) and *DNAH11* ciliopathy (Pan et al. 1998; Bartoloni et al. 2002). One patient had congenital chloride diarrhea (Hoglund et al. 1994). Two of seven patients had an unexplained developmental delay (Fares et al. 2006; Feuk et al. 2006). One of the patients with UPD(7)pat and CF also presented with hyperbilirubinemia and a cholestatic pattern lasting for several

months, in addition to postnatal overgrowth and delayed development (Fares et al. 2006). All but two were molecularly confirmed complete isodisomies (Feuk et al. 2006; Goh et al. 2007). In addition, a study on methylation profiling in UPD included two individuals with UPD(7)pat without phenotype information (Joshi et al. 2016), and furthermore there were three UPD(7)pat individuals found in a large population screen (Nakka et al. 2019). An overview also including nonpublished UPD(7)pat patients can be found at http://cs-tl.de/DB/CA/UPD/7-UPDp.html.

Mosaic segmental paternal UPD11p is a common cause of Beckwith–Wiedemann spectrum overgrowth disorders (BWSp). Other causes of BWSp are loss of methylation (LOM) of imprinting center 2 (*CDKNC1/KCNQ1*), gain of methylation (GOM) of imprinting center 1 (*H19/IGF2*), and mutations in the imprinting centers or the growth-inhibitor *CDKN1C*.

Complete genome-wide paternal UPD (GWpUPD), also called uniparental diploidy, is lethal and associated with a molar pregnancy, whereas mosaic GWpUPD, also called androgenetic/biparental chimerism, has been reported more than 30 times in the literature. Low-level mosaicism with tissue variations can be difficult to detect (Kalish et al. 2013; Christesen et al. 2020). Clinical features include placental mesenchymal dysplasia (PMD) and placentomegaly, BWSp, hyperinsulinism, capillary hemangiomas, elevated risk of cancer, and signs of mosaicisms like lateralized overgrowth (Kotzot 2008; Kalish et al. 2013; Postema et al. 2019; Sheppard et al. 2019). However, signs of other imprinting disorders like Angelman syndrome can sometimes be evident (Inbar-Feigenberg et al. 2013; Sheppard et al. 2019; Christesen et al. 2020). Conjugated hyperbilirubinemia is not established as a feature of imprinting disorders. However, this was documented in five girls with mosaic GWpUPD and a BWS-like phenotype with hyperinsulinism (Kalish et al. 2013; Lee et al. 2019; Christesen et al. 2020), in one case of UPD(6)pat (other methylation defects or UPDs were not ruled out in this patient) (Kenny et al. 2009), and in one case of UPD(7)pat (Fares et al. 2006).

We report on a young boy who initially presented with a phenotype overlapping BWSp and GWpUPD, but with the surprising finding of a double paternal isodisomy of the imprinted Chromosomes 7 and 15. A case of two concurrent UPDs in the same individual has not been clinically described previously. Therefore, we wanted to investigate if the double UPDs affected the transcription of other imprinted genes. We discuss the most likely mechanism of origin, suggest that paternal UPD7 might not be phenotypically neutral, and explore the gene expression pattern in patient fibroblast to find an explanation for the phenotype.

RESULTS

Clinical Presentation and Family History

The boy was born from unrelated healthy parents; the mother described the pregnancy as problematic compared to her former pregnancy, and she developed cravings for carbohydrates and felt tired constantly. Still, there were no complications and three regular ultrasound scans. Nuchal translucency was normal (1.26 mm) at gestation week 12 + 1. Spontaneous vaginal birth took place at gestation week 40 + 5, with Apgar scores 9/9/10 after 1, 5, and 10 min. He was 57 cm (2.98 SD) and weighed 4540 g (1.79 SD) at birth; head circumference was 0 SD the first week, and all growth references are according to Norwegian children growth charts (Juliusson et al. 2009). Placentomegaly with an untrimmed weight of 1.7 kg was noted, but unfortunately the placenta was not further examined. The boy was admitted to intensive care after 1.5 h as a result of hypoglycemia (lowest level 1.6 mmol/L). He developed jaundice and was diagnosed with conjugated hyperbilirubinemia, peaking at 7 wk of age with conjugated bilirubin of 109 μmol/L (<5) and elevated liver transaminases. After that, the bilirubin slowly decreased to normal levels at

4–6 mo of age, after which all medical supplements (ursodeoxycholic acid, fat-soluble vitamins) were withdrawn. Because of prolonged hypoglycemia and high insulin levels in the blood, he was diagnosed with transient hyperinsulinism that lasted 5–6 wk. He had a systolic heart murmur and clinically enlarged spleen and liver (4–5 cm below costal margin). Small palpable occipital skin tumors were present at birth, and ultrasound examination suggested hemangiomas. These disappeared within the first month of life. Regarding BWSp features, he had bilateral earlobe creases (Supplemental Fig. S1) but no asymmetry, umbilical hernia, or macroglossia. Abdominal ultrasound showed large and hyper-echogenic kidneys bilaterally, slightly enlarged normal liver, and normal pancreas and spleen, also confirmed in later scans. Echocardiography and neonatal electroencephalogram (EEG) were normal and so was an X-ray of the chest and spinal column. Explorative laparotomy and cholangiography at 5 wk of age were normal. Still, a liver biopsy revealed a possible paucity of intrahepatic bile ducts and cholestasis with minimal inflammation, no glycogenosis, and a diploid status (Haroske et al. 2001). His hyperbilirubinemia was considered secondary to hyperinsulinism. Head circumference fell from 0 SD to −1.2 SD at 10 mo of age. Height at 10 mo of age was 2.4 SD and weight 4.0 SD. He smiled at 5 wk of age and could roll over from his back at 3.5 mo. Breastfeeding was unsuccessful, but otherwise there were no feeding difficulties. At 11 mo of age, he was a happy baby with mild sleeping problems and constipation, and bilateral inguinal testes were found. There were no dysmorphic features, and he had frequent smiles, strabismus, full cheeks, no words, played with toys using both hands, could sit without support for a short period, and moved around freely by shuffling on all fours. He had moderately delayed motor milestones, but he was too young for formal assessment.

The family history was negative. Both parents were tall and slim, the father was 36 yr and 190 cm, and 54 cm and 4.25 kg at birth. The mother was 42 yr and 180 cm, and she was 3572 g at birth, 4 wk preterm. A healthy elder sister was 53 cm and 3740 g at birth, with a placenta of 520 g (trimmed weight of 394 g without fetal membranes and umbilical cord, corresponding to the 10th centile for 39 wk gestation).

The clinical scoring system of BWSp requires a minimum of four points (Brioude et al. 2018), and he scored five points—two points for hyperinsulinism lasting >1 wk, and three points from suggestive features: placentomegaly, ear creases, and nephromegaly and hepatomegaly. According to Norwegian growth charts, his birth weight of 4.45 kg is 1.79 SD, but according to World Health Organization (WHO) references, his birth weight was 2.2 SD, and this would have added another suggestive point and a total BWSp score of 6.

Diagnostic Workup

Just after birth, methylation-specific (MS) multiplex ligation-dependent probe amplification (MLPA) ME030-C1 (BWS) test, an arrayCGH test (on a 180K Agilent array), and an next-generation sequencing (NGS)-based gene panel test with genes associated with liver diseases and hyperinsulinism were performed with normal results. At admission to our hospital because of hyperinsulinism at 5 wk of age, we performed a CytoScanHD Array that revealed complete isodisomy of both Chromosomes 7 and 15, but no (likely) pathogenic copy-number variants (CNVs). As he presented with neither hypotonia (seen in PWS/UPD(15)mat) nor growth restriction (seen in Silver–Russell/UPD(7)mat), we suspected both iUPDs to be paternal or possibly representing clonal mosaicism restricted to peripheral blood. An MS-MLPA test on DNA from a separate blood sample confirmed that both UPDs were paternal, with complete LOM of *MEST/GRB10* in 7q32 and *MAGEL2/SNRP/UBE3A* in 15q11.2. Methylation patterns in differentially methylated regions (DMRs) on Chromosomes 6, 11, and 14 were normal. Trio-based whole-exome sequencing (WES) gave normal results without evidence for recessive, de novo, X-linked or imprinting

disorders and confirmed lack of biparental inheritance of single-nucleotide variants (SNVs) on Chromosomes 7 and 15. Also, *ABCC8* MLPA and *CDKN1C* Sanger sequencing were normal.

We wanted to exclude a clonal UPD event, aneuploidy-mosaicism, or GWpUPD. Chromosome analysis confirmed a normal male karyotype 46,XY in the blood (70 metaphases) and cultured skin fibroblast (39 metaphases) from a skin biopsy taken at 5 mo of age. In addition, fluorescence in situ hybridization (FISH) analysis of centromeres X and Y in 100 interphase nuclei from peripheral blood leukocytes was normal. We also repeated all three relevant MS-MLPA analyses in DNA extracted directly from the skin biopsy, with identical results to blood DNA. Parental karyotypes were both normal.

Karyotype 46,XY.arr[GRCh37] 7p22.3q36.3(44166_159119220)x2 hmz pat,
15q11.2 q26.3(22752398_102429049)x2 hmz pat

RNA Analysis

As his BWSp phenotype did not correlate with the molecular findings, RNA-seq was performed on fibroblast RNA to explore the expression of imprinted genes and other genes of interest, particularly genes involved in growth. We compared this patient to fibroblast RNA-seq results from six control samples. The results are summarized in Supplemental Table S1. Of the approximately 64,000 genes analyzed, which included alternative assemblies, 11,299 genes passed quality checks. Of these, 103 genes were up-regulated (fold change [FC] > 2), of which 99 were protein-coding genes. Similarly, 27 genes were down-regulated (FC < 0.5), of which 15 were protein-coding. There were only four imprinted differentially expressed genes (DEGs), all up-regulated. One of these (*NAP1L4)* is annotated with an unknown imprinting status, one (*PKP3*) has a predicted maternal expression, and two (*DIRAS3* and *PEG10*) had paternal expression. This analysis yielded no down-regulated imprinted gene. Gene sets that were significantly enriched (adjusted *P*-value <0.05) with DEGs fulfilling both the quality and FC criteria described above are listed in Supplemental Table

Table 1. Results from RNA expression analysis of up- or down-regulated imprinted genes on Chromosomes 7 and 15

Gene	Ensembl GeneName	Chr	FC_Index- MedianCtrls	SD	FC_{min} (>2)	FC_{max}	log_2FC	Expressed allele
PEG10	ENSG00000002746	Chr 7	6.55	2.77	4.43	12.09	2.71	Paternal
NDN	ENSG00000105825	Chr 15	2.31	1.21	*1.49*	4.61	1.21	Paternal
GLI3	ENSG00000206190	Chr 7	2.07	0.91	*0.68*	3.39	1.05	Paternal
SGCE	ENSG00000135211	Chr 7	1.59	0.36	*0.88*	1.92	0.67	Paternal
SNRPN	ENSG00000187391	Chr 15	1.54	0.47	*0.76*	1.98	0.62	Paternal
RAC1	ENSG00000158623	Chr 7	1.22	0.21	*1.06*	1.64	0.29	
UBE3A	ENSG00000106070	Chr 15	1.14	0.17	*0.85*	1.31	0.18	Maternal
CCDC71L	ENSG00000164896	Chr 7	0.87	0.18	*0.77*	1.22	−0.20	Paternal
GRB10	ENSG00000114062	Chr 7	0.81	0.17	*0.55*	0.99	−0.30	Isoform-dependent
MAGI2	ENSG00000128739	Chr 7	0.75	0.45	*0.21*	1.29	−0.42	Maternal
ATP10A	ENSG00000106571	Chr 15	0.67	0.19	*0.37*	0.86	−0.58	Maternal
TFPI2	ENSG00000182636	Chr 7	0.45	5.02	*0.16*	10.68	−1.16	Maternal
HECW1	ENSG00000242265	Chr 7	0.23	0.16	*0.17*	0.61	−2.15	Paternal

We only present genes passing the quality check with normalized RNA expression value >8 (see Supplemental Table S1). FC_Index-MedianCtrl represents the fold change between the normalized expression value of the index patient and the median normalized expression value of the six controls. FC_Min (>2) is the lowest fold change between the index and a control sample; genes not fulfilling criteria of an FC_Min >2 are marked with FC_Min in italics. FC_Max is the largest fold change between the index and a control sample.
(FC) Fold change, (Chr) corresponding chromosomal locus, (SD) standard deviation.

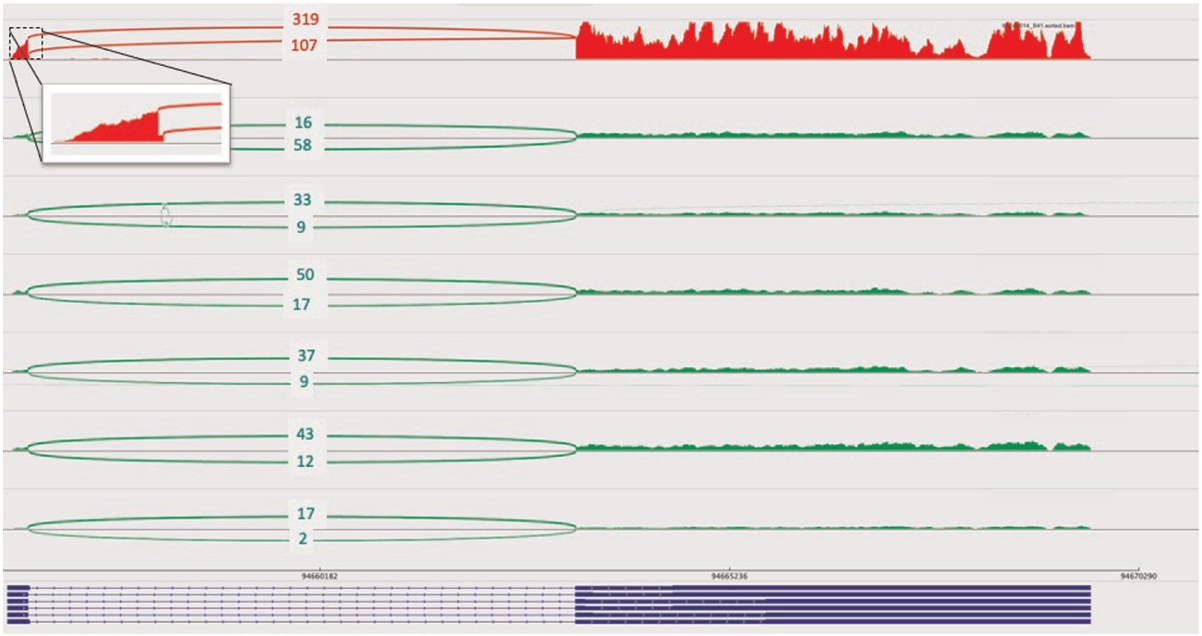

Figure 1. The Sashimi plot (IGV 2.3.74) of *PEG10* RNA-seq analysis displaying the two open reading frames (ORFs) with 11 nt difference between the two consecutive intron 1 donor sites, comparing the expression level in the index (red) to controls (green).

S1. Two relevant gene sets for growth (marked in bold) were both enriched for up-regulated genes, and according to these gene sets, 11/103 (11%) of up-regulated genes were involved in growth.

Finally, we looked at the expression status of (tentative) imprinted genes on Chromosomes 7 and 15, passing the quality check irrespectively of FC, but excluding genes with only predicted or conflicting data (Table 1). *MEST* did not pass quality criteria in five out of six controls and therefore is not included in the table. In summary, we show that the five genes with the highest FC were all paternally imprinted. No significant expression change in BWS genes like *IGF2* and *CDKN1C* was evident. *PEG10* with an FC of 6.55 and FC_min of 4.43 was the only gene also passing the FC > 2 criteria. This gene has two open reading frames (ORFs). We find ~3× higher expression for the most extended transcript in both index and controls, visualized as a Sashimi plot in Figure 1. Exon 1–intron 1 junction is shown on a large scale, confirming that in ORF1, intron 1 is 11 nt longer than in ORF2. The number of tracks spanning splice junctions is shown.

DISCUSSION

In a baby boy with a BWSp-like phenotype, we detected double paternal iUPD7 and iUPD15 (a cause of Angelman syndrome), none of which is known to affect intrauterine growth. The clinical BWSp suspicion, despite normal genetic and imprinting status for BWS locus, pointed to the existence of an "imprinted gene network" (IGN), in which imprinted genes can influence the expression of other imprinted genes even when on other chromosomes (Patten et al. 2016; Eggermann et al. 2021). Six reported patients with concurrent UPD and imprinting defects involving loci on other chromosomes provide further support to the IGN hypothesis (Arima et al. 2005; Begemann et al. 2012; Hara-Isono et al. 2020; Choufani et al. 2021).

Nevertheless, this was not confirmed by RNA-seq in our case. Therefore, we suggest that his phenotype was attributed to his double UPDs, through imprinting defects or up-regulation of nonimprinted genes involved in growth (Table 1; Supplemental Table S1). By definition, the boy has a multilocus imprinting disorder (MLID). It is possible that all MLID with paternal methylation patterns could lead to a BWSp-like phenotype, regardless of which DMRs are involved, but it is also possible that overexpression of the paternally imprinted gene *PEG10* on Chromosome 7 is growth-promoting (Fig. 1).

Overlapping phenotypic features of many imprinting disorders—in particular, SRS (LOM H19/IGF2:IG-DMR on 11p15.5), Temple syndrome (TS) (LOM DLK1/MEG3:IG-DMR on 14q32.2), and PWS (GOM SNURF:TSS-DMR on 15q11q13)—also support the IGN notion. However, genome-wide methylome analyses in these three patient groups have not revealed any apparent relationships between the methylation pattern and the shared phenotypic expression in these patients (Hara-Isono et al. 2020). In contrast, transcriptome analysis performed in patients with TS, SRS, and one mixed TS and SRS showed some overlapping features such as decreased *IGF2* expression, and TS and PWS patients showed decreased *SNURF* expression (Abi Habib et al. 2019).

Most imprinted DEGs on Chromosomes 7 and 15 in the boy showed expression changes as expected from the imprinting pattern (Table 1). *UBEA3A* shows slightly increased expression but below our fold change criteria. However, this gene is biallelically expressed in fibroblasts and only maternally expressed in the brain. The imprinting status is documented only in the placenta for the paternally expressed down-regulated genes *CCDC71L* and *HECW1* (Sanchez-Delgado et al. 2015).

In conclusion, we did not identify a single or a group of DEGs explaining the placentomegaly or overgrowth in the boy apart from high expression of *PEG10* nor a general dysregulation of known imprinted disease genes (Table 1). However, we found significant enrichment for up-regulated genes in gene sets associated with growth and, in general, about four times as many up-regulated as down-regulated DEGs.

Clinical findings were reminiscent of BWSp or mosaic GWpUPDs, which were molecularly excluded. A large placenta is a hallmark of BWS, but weight >1 kg is uncommon and a placenta of 1.9 kg has been reported in GWpUPD (Postema et al. 2019). Unfortunately, placental tissue and pathology were not available. Of note, iUPD(7)pat in postnatal overgrowth and a large and fused twin placenta of 1340 g at gestation week 34 has been reported (Nakamura et al. 2018). A partly phenotypic overlap was also found in a patient with cystic fibrosis due to iUPD(7)pat, hyperbilirubinemia with cholestatic pattern, and postnatal overgrowth (Fares et al. 2006). The imprinted genes *GRB10* on 7p12 and *MEST* (*PEG1*) on 7q32 have been suggested to be implicated in growth restriction (Carrera et al. 2016; Eggermann et al. 2019). A potential role in overgrowth in UPD(7)pat has also been discussed (Nakamura et al. 2018), and BWSp features was noted in a patient with a maternal *GRB10* deletion (Naik et al. 2011). Our study showed increased *PEG10* expression above the expected doubling from UPD, with a sixfold change (Table 1), whereas *GRB10* was not significantly down-regulated (FCmedian 0.81). Unfortunately, *MEST* did not pass quality control; thus, our study is inconclusive on the regulation on *MEST* expression. We speculate that *PEG10* (paternally expressed gene 10) on 7q21.3 might be a cause of both the fetal and placental overgrowth, being a known oncogene (Xie et al. 2018) and essential for placental development (Ono et al. 2006; Abed et al. 2019). This is in line with an SRS phenotype with normal-sized placentas in two patients with paternal isochromosomes 7p combined with maternal isochromosomes 7q (Eggerding et al. 1994; Kotzot et al. 2001). *PEG10* has two conserved ORFs (Xie et al. 2018), also confirmed by RNA-seq. *PEG10* is strongly expressed in the placenta, but also shows high expression in kidneys, lung, brain, and endocrine tissues, and it is involved in cancer proliferation, apoptosis, and metastasis.

Conjugated hyperbilirubinemia has been reported in eight patients with UPD, and 7/8 presented with hyperinsulinism. Hyperinsulinemic hypoglycemia is associated with spontaneously resolving conjugated hyperbilirubinemia in newborns (Edwards et al. 2021). A systematic review of 1692 subjects with conjugated hyperbilirubinemia in infancy does not describe any patients with UPD (Gottesman et al. 2015). Furthermore, NGS and CNV analysis did not reveal other causes of bilirubinemia in the boy. Although these methods have limitations, the clinical findings and transient and benign nature correspond well with the description of hyperbilirubinemia in UPD patients in the literature. Our report demonstrates that UPDs could very well be overlooked in patients with conjugated hyperbilirubinemia, as the UPD diagnosis in the boy was missed in the first hospital.

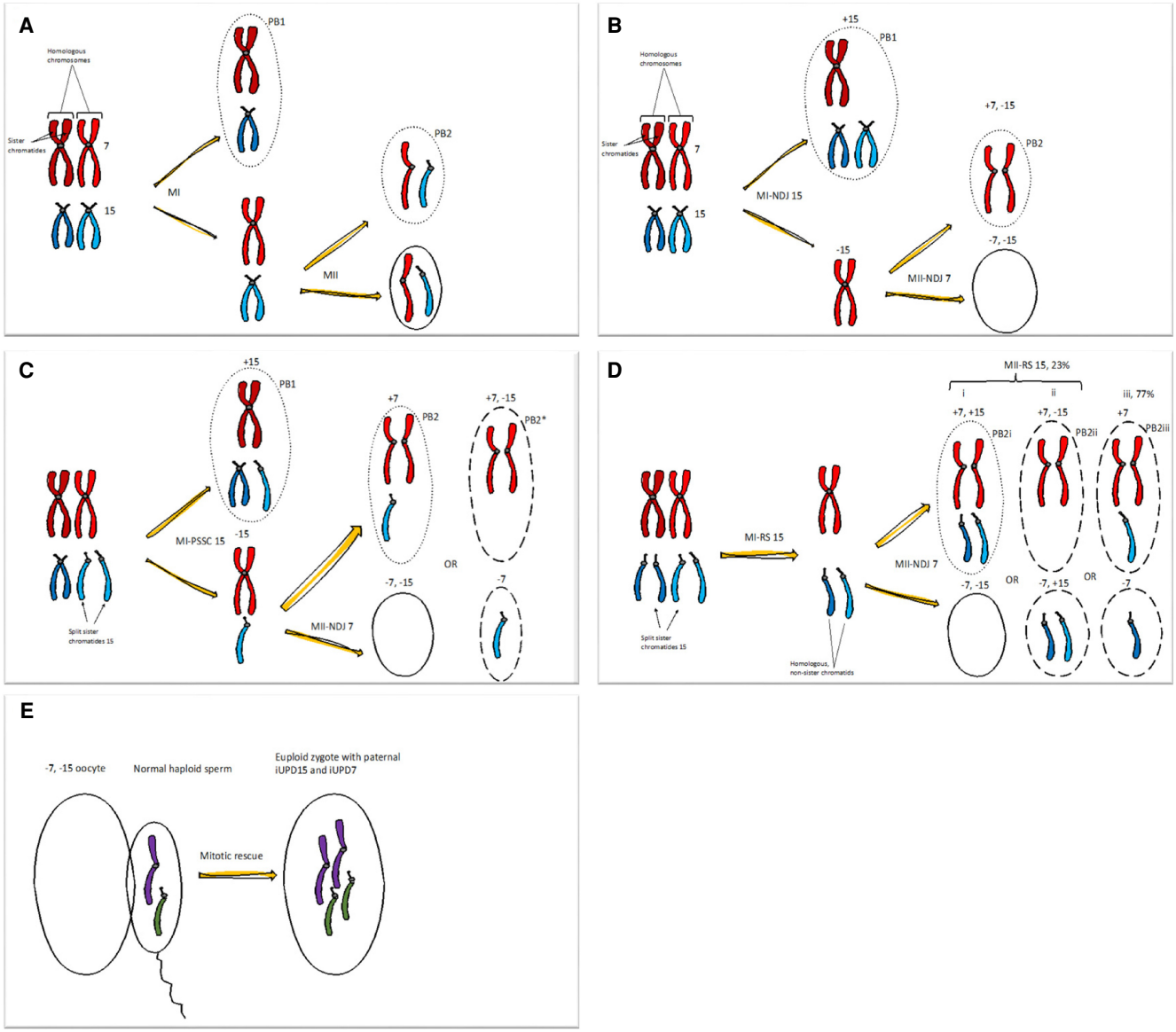

Figure 2. Abnormal female meiosis resulting in a double nullisomic oocyte, in which alternative *C* or *D* is the most likely event in our case. (*Legend continued on following page.*)

In Figure 2, we have outlined the most plausible segregation errors causing double iUPD. Because paternally derived aneuploidies are very rare, causing <1% of all meiotic errors (Tyc et al. 2020), a maternal origin of the double UPD was most likely (e.g., a correction of a double maternal monosomy). This was found in 4%–6% of the blastomeres at maternal age 40–42 yr (Tyc et al. 2020). Furthermore, an initial meiosis I (MI) error in oocytes increased the probability of a subsequent meiosis II (MII) error like nondisjunction (NDJ) by ~2.2-fold. The initial meiotic error could be of NDJ type, but premature separation (and missegregation) of sister chromatids (PSSC) (Fig. 2C) and reverse segregation are both more prevalent, particularly in advanced maternal age (Ottolini et al. 2015; Capalbo et al. 2017; Gruhn et al. 2019). Gamete complementation (a double disomic sperm meeting a double nullisomic ovum) is improbable. Complex mitotic errors are eradicated very early in embryo development. In contrast, meiotic errors are more prone to persist (McCoy et al. 2015). Thus, the most likely origin of the double paternal UPD is maternal double monosomy, causally related to increased maternal age. The meiotic errors probably involved a PSSC in MI, resulting in monosomy 15, or, alternatively, reverse segregation of Chromosome 15 in MI with missegregation in MII. The aneuploid MI oocyte was susceptible to MII-NDJ, affecting Chromosome 7. Postzygotic monosomy rescue with paternal isodisomy of both Chromosomes 15 and 7 then occurred, with a total loss of monosomic cell lines.

In conclusion, we describe for the first time a child with double paternal isodisomy UPD 7 and 15, presenting with Angelman syndrome and a Beckwith–Wiedemann spectrum phenotype. We did not find an alternative explanation for the BWSp phenotype by WES, methylation testing, and RNA-seq, but we suggest that overexpression of *PEG10* could be related

Figure 2. (*Continued.*) (*A*) Normal situation with canonical meiotic division I and II with normal segregation of Chromosomes 7 (red) and 15 (blue). The first meiotic division separates the pair of homologous chromosomes, whereas the second division separates sister chromatids. Dotted lines represent polar bodies (PB), and complete lines the oocyte. Recombinations are omitted from the figures for simplicity. (MI) Meiosis I, (MII) meiosis II. (*B*) Canonical MI and MII with nondisjunction (NDJ). At MI, homologous chromosomes should segregate to opposite spindle pools, but here the homologous Chromosome 15 missegregate. Chromosome 15 is the most frequent chromosome involved in aneuploidy and also represents the chromosomes with the strongest maternal age effect on premature separation (and missegregation) of sister chromatids (PSSC) and reverse segregation (RS) (McCoy et al. 2015; Capalbo et al. 2017; Gruhn et al. 2019). In an aneuploid oocyte, the risk of MII-NDJ increases, here depicted with NDJ of Chromosome 7, where the sister chromatids fail to separate. The double nullisomy oocyte (−7, −15) outcome is outlined. Polar body 1 (PB1) from MI-NDJ show +15 (disomy 15), and PB2 (dotted line) show +7, −15 (mixed disomy and nullisomy). The result from MII-NDJ of Chromosome 7 in an oocyte with a PB1 constitution is not drawn but would be +7,+15 (double disomy) and −7, +15 (mixed nullisomy and disomy). (*C*) Meiosis with premature (or precocious) separation of sister chromatids (PSSC), in which sister chromatids of one Chromosome 15 loose cohesins and split prematurely and separate in MI, forming a free chromatid, and segregate with (PB1, +15) or without (−15) the homologous chromosome. In addition, we include MII-NDJ of Chromosome 7. Chromatid 15 can be expelled into PB2 (+7) in MII, making a nullisomic oocyte (−7, −15). This chromatid could also stay in the oocyte during MII; see the dashed outlines of the alternative oocyte (−7) and PB2* (+7, −15). (*D*) Noncanonical meiosis with reverse segregation (RS), in which sister chromatids of Chromosome 15 segregate to different primary oocytes in MI, and homologous chromatids segregate in MII (*iii*). For simplicity, we have drawn only one of the two outcomes and also omitted PB1. RS of Chromosome 15 occurs in MI, and the three possible MII outcomes depicted all show MII-NDJ of Chromosome 7. An additional RS-MII error of the non-sister chromatids 15 occurs in the first two alternatives (*i* and *ii*), and balanced segregation of 15 in the last (*iii*). According to Ottolini et al. (2015) MI-RS error with missegregation of the non-sister chromatids into the same oocyte in MII (*i* and *ii*) will occur in 23%. We have outlined the double nullisomic oocyte; the corresponding PB2 is marked with dots (*i*), and alternative oocytes and PB2s (*ii*, *iii*) with dashes. (*E*) Fertilization with a balanced haploid sperm, followed by postzygotic double monosomy rescue via endoduplication in the zygote, producing a double paternal isodisomy of Chromosomes 7 and 15. Maternal MII completion, including extrusion of PB2, occurs after fertilization with the haploid sperm, but this is drawn separately for simplicity.

to large placental and body size. Even though clinically suspected, we could not confirm an imprinted gene network.

METHODS

DNA and RNA Isolation

DNA extracted from peripheral blood from the boy drawn at 5 wk of age was used for most analyses. DNA extracted from uncultivated fibroblasts from a skin biopsy taken at 5 mo of age was used to confirm the initial molecular analysis. RNA was extracted from cultivated fibroblasts from the same skin biopsy using the RNeasy Mini Kit (QIAGEN) and Tape station RIN value of 10. We performed chromosome analysis with conventional karyotyping and interphase FISH analysis on peripheral heparin blood and skin biopsy.

CNV, Methylation, and NGS Analysis

DNA isolated from peripheral blood and fibroblasts from the proband was analyzed for relevant CNVs and methylation aberrations by SALSA MLPA probemix ME030 BWS/RSS version C3, ME032 UPD7–UPD14 version A1, ME028 PWS/AS version C1, and P117 *ABCC8* version C2 (MRC-Holland). Also, we tested DNA from the blood for imprinted loci on Chromosomes 6 and 14 by using the ME032 kit and for genomic CNVs and long stretches of homozygosity by CytoScanHD Array (Thermo Fisher Scientific). We performed NGS analysis (trio-WES) as earlier published (Berland et al. 2020).

RNA Sequencing

We purified total RNA from cultured fibroblasts from the boy's skin biopsy. A whole transcriptome sequencing library was generated using the Illumina TruSeq Stranded Total RNA kit with Ribo-Zero Gold depletion for fibroblasts, according to the manufacturer's protocols. We quality checked the library on the Agilent Bioanalyzer system (RIN > 9) and accurately quantified it using the KAPA qPCR quantification kit. The library was paired-end sequenced on the Illumina HiSeq4000 system with a read length of 2 × 75 nt and a depth of approximately 100 million reads. RNA-seq reads were aligned to the human genome reference (assembly GRCh38.p10) using HISAT2 (v2.0.5) (Kim et al. 2015; Pertea et al. 2016). Reads aligned within the coding part of the genome (adequate GENCODE v25 gene annotation file) were counted using featureCounts (Liao et al. 2014). Read counts were further normalized and analyzed for differential expression compared to six samples from another run (three adult women and three young boys aged 5–16 yr) using DESeq2 (Love et al. 2014) with default options in the R/Bioconductor environment (Gentleman et al. 2004). We visualized data in IGV (Integrative Genomics Viewer v2.3.74). Genes were annotated by FUMA (Functional Mapping and Annotation; https://fuma.ctglab.nl/) GENE2FUNC software (Watanabe et al. 2017), and enrichment analyses were performed by GSEA software (Broad Institute; http://www.gsea-msigdb.org/gsea/index.jsp) (Subramanian et al. 2005).

RNA-seq Expression Analysis

For differential expression analysis and estimation of the fold change of RNA-seq count data, we used DESeq2, which performs an internal normalization in which we calculate a geometric mean for each gene across all samples (Love et al. 2014). The gene counts for a gene in each sample are then divided by this mean. The median of these ratios in a sample is the size factor for that sample. This procedure corrects for library size and RNA composition bias, which can arise, for example, when only a small number of genes are highly expressed in one experiment condition but not in the other. The logarithmic fold change can be viewed

as effect size and account for noisiness from genes with low expression (few counts). FC of the RNA expression level is defined as $2^{(\text{sample-controls})}$. In this case, we used the median normalized expression of all controls; $FC = 2^{(\text{ExprIndex} - \text{MedExprCtrls})}$. Genes with normalized expression data values > 8 have adequate quality and were included in further analysis. We have data from six controls; none had overlapping phenotypes, UPDs, or pathogenic CNVs, and two adults are considered entirely healthy (Supplemental Table S2). For further analysis, we only included DEGs fulfilling stringent criteria; up-regulated DEGs with $FC > 2$ and $FCmin \geq 2$, implying that all individual FC_Index-Ctrl must be ≥2, and down-regulated DEGs with $FC < 0.5$ but also $FCmax\_Index\text{-}Ctrl \leq 0.5$. We collected gene sets from http://geneontology.org/, and a list of 256 imprinted or predicted imprinted genes from https://www.geneimprint.com/site/genes-by-species in June 2021 to analyze up-regulated or down-regulated DEGs.

ADDITIONAL INFORMATION

Data Deposition and Access

Consent was not obtained to make the patient's or the control's raw DNA or RNA sequencing data publicly available.

Ethics Statement

Genetic analysis for this family was performed as clinical testing in a diagnostic setting; transcriptional analysis was performed as part of an overall assessment for interpretation of the findings. This study was undertaken as part of the clinical workup at the Department of Medical Genetics at Haukeland University Hospital, Bergen. Informed consent from the parents for publication of the family history and photographs is stored in the patient's files as a secure archive and to ensure the anonymity of the family.

Acknowledgments

We are most grateful to the family whose enthusiastic collaboration was essential to do such a complex genetic study. We also thank our coworkers Rita Holdhus, Tomasz Stokowy, Hilde Rusaas, and Sigrid Erdal, and we acknowledge the service from the Genomic Core Facility (GCF) at the University of Bergen, which is supported by Trond Mohn Foundation, for promoting the RNA sequencing.

Author Contributions

S.B., G.H., and B.I.H. designed the study. S.B., M.H.L.B., E.J.W., and C.F.R. examined, investigated, and cared for the patient and the family. G.T. examined and analyzed the liver biopsy and provided information on sibling's placenta. B.I.H. supervised the RNA-seq. S.B., S.J., G.H., and B.I.H. analyzed the data. S.J., G.H., and B.I.H. supervised the work. S.B. wrote and submitted the manuscript. All authors reviewed and provided input for the manuscript. All authors declare no conflicts of interest and have read and approved the manuscript and its submission.

Competing Interest Statement

The authors have declared no competing interest.

Received July 8, 2021; accepted in revised form August 31, 2021.

REFERENCES

Abed M, Verschueren E, Budayeva H, Liu P, Kirkpatrick DS, Reja R, Kummerfeld SK, Webster JD, Gierke S, Reichelt M, et al. 2019. The Gag protein PEG10 binds to RNA and regulates trophoblast stem cell lineage specification. *PLoS ONE* **14:** e0214110. doi:10.1371/journal.pone.0214110

Habib W A, Brioude F, Azzi S, Rossignol S, Linglart A, Sobrier ML, Giabicani E, Steunou V, Harbison MD, Le Bouc Y, et al. 2019. Transcriptional profiling at the *DLK1/MEG3* domain explains clinical overlap between imprinting disorders. *Sci Adv* **5:** eaau9425. doi:10.1126/sciadv.aau9425

Arima T, Kamikihara T, Hayashida T, Kato K, Inoue T, Shirayoshi Y, Oshimura M, Soejima H, Mukai T, Wake N. 2005. *ZAC*, *LIT1* (*KCNQ1OT1*) and *p57^{KIP2} (CDKN1C)* are in an imprinted gene network that may play a role in Beckwith–Wiedemann syndrome. *Nucleic Acids Res* **33:** 2650–2660. doi:10.1093/nar/gki555

Bartoloni L, Blouin JL, Pan Y, Gehrig C, Maiti AK, Scamuffa N, Rossier C, Jorissen M, Armengot M, Meeks M, et al. 2002. Mutations in the *DNAH11* (axonemal heavy chain dynein type 11) gene cause one form of situs inversus totalis and most likely primary ciliary dyskinesia. *Proc Natl Acad Sci* **99:** 10282–10286. doi:10.1073/pnas.152337699

Begemann M, Spengler S, Kordaβ U, Schröder C, Eggermann T. 2012. Segmental maternal uniparental disomy 7q associated with *DLK1/GTL2* (14q32) hypomethylation. *Am J Med Genet A* **158A:** 423–428. doi:10.1002/ajmg.a.34412

Berland S, Haukanes BI, Juliusson PB, Houge G. 2020. Deep exploration of a *CDKN1C* mutation causing a mixture of Beckwith–Wiedemann and IMAGe syndromes revealed a novel transcript associated with developmental delay. *J Med Genet* doi:10.1136/jmedgenet-2020-107401

Brioude F, Kalish JM, Mussa A, Foster AC, Bliek J, Ferrero GB, Boonen SE, Cole T, Baker R, Bertoletti M, et al. 2018. Expert consensus document: clinical and molecular diagnosis, screening and management of Beckwith–Wiedemann syndrome: an international consensus statement. *Nat Rev Endocrinol* **14:** 229–249. doi:10.1038/nrendo.2017.166

Capalbo A, Hoffmann ER, Cimadomo D, Ubaldi FM, Rienzi L. 2017. Human female meiosis revised: new insights into the mechanisms of chromosome segregation and aneuploidies from advanced genomics and time-lapse imaging. *Hum Reprod Update* **23:** 706–722. doi:10.1093/humupd/dmx026

Carrera IA, de Zaldívar MS, Martín R, Begemann M, Soellner L, Eggermann T. 2016. Microdeletions of the 7q32.2 imprinted region are associated with Silver–Russell syndrome features. *Am J Med Genet A* **170:** 743–749. doi:10.1002/ajmg.a.37492

Choufani S, Ko JM, Lou Y, Shuman C, Fishman L, Weksberg R. 2021. Paternal uniparental disomy of the entire chromosome 20 in a child with Beckwith–Wiedemann syndrome. *Genes (Basel)* **12:** 172. doi:10.3390/genes12020172

Christesen HT, Christensen LG, Löfgren AM, Brøndum-Nielsen K, Svensson J, Brusgaard K, Samuelsson S, Elfving M, Jonson T, Gronskov K, et al. 2020. Tissue variations of mosaic genome-wide paternal uniparental disomy and phenotype of multi-syndromal congenital hyperinsulinism. *Eur J Med Genet* **63:** 103632. doi:10.1016/j.ejmg.2019.02.004

den Besten I, de Jong RF, Geerts-Haages A, Bruggenwirth HT, Koopmans M, ENCORE Expertise Center for AS 18+, Brooks A, Elgersma Y, Festen DAM, Valstar MJ. 2021. Clinical aspects of a large group of adults with Angelman syndrome. *Am J Med Genet A* **185:** 168–181. doi:10.1002/ajmg.a.61940

Edwards M, Falzone N, Harrington J. 2021. Conjugated hyperbilirubinemia among infants with hyperinsulinemic hypoglycemia. *Eur J Pediatr* **180:** 1653–1657. doi:10.1007/s00431-021-03944-0

Eggerding FA, Schonberg SA, Chehab FF, Norton ME, Cox VA, Epstein CJ. 1994. Uniparental isodisomy for paternal 7p and maternal 7q in a child with growth retardation. *Am J Hum Genet* **55:** 253–265.

Eggermann T, Begemann M, Kurth I, Elbracht M. 2019. Contribution of *GRB10* to the prenatal phenotype in Silver–Russell syndrome? Lessons from 7p12 copy number variations. *Eur J Med Genet* **62:** 103671. doi:10.1016/j.ejmg.2019.103671

Eggermann T, Davies JH, Tauber M, van den Akker E, Hokken-Koelega A, Johansson G, Netchine I. 2021. Growth restriction and genomic imprinting-overlapping phenotypes support the concept of an imprinting network. *Genes (Basel)* **12:** 585. doi:10.3390/genes12040585

Engel E. 1980. A new genetic concept: uniparental disomy and its potential effect, isodisomy. *Am J Med Genet* **6:** 137–143. doi:10.1002/ajmg.1320060207

Engel E. 2006. A fascination with chromosome rescue in uniparental disomy: Mendelian recessive outlaws and imprinting copyrights infringements. *Eur J Hum Genet* **14:** 1158–1169. doi:10.1038/sj.ejhg.5201619

Fares F, David M, Lerner A, Diukman R, Lerer I, Abeliovich D, Rivlin J. 2006. Paternal isodisomy of Chromosome 7 with cystic fibrosis and overgrowth. *Am J Med Genet A* **140:** 1785–1788. doi:10.1002/ajmg.a.31380

Feuk L, Kalervo A, Lipsanen-Nyman M, Skaug J, Nakabayashi K, Finucane B, Hartung D, Innes M, Kerem B, Nowaczyk MJ, et al. 2006. Absence of a paternally inherited *FOXP2* gene in developmental verbal dyspraxia. *Am J Hum Genet* **79:** 965–972. doi:10.1086/508902

Gentleman RC, Carey VJ, Bates DM, Bolstad B, Dettling M, Dudoit S, Ellis B, Gautier L, Ge Y, Gentry J, et al. 2004. Bioconductor: open software development for computational biology and bioinformatics. *Genome Biol* **5:** R80. doi:10.1186/gb-2004-5-10-r80

Goh DL, Zhou Y, Chong SS, Ngiam NS, Goh DY. 2007. Novel *CFTR* gene mutation in a patient with CBAVD. *J Cyst Fibros* **6:** 423–425. doi:10.1016/j.jcf.2007.02.004

Gottesman LE, Del Vecchio MT, Aronoff SC. 2015. Etiologies of conjugated hyperbilirubinemia in infancy: a systematic review of 1692 subjects. *BMC Pediatr* **15:** 192. doi:10.1186/s12887-015-0506-5

Grugni G, Crino A, Bosio L, Corrias A, Cuttini M, De Toni T, Di Battista E, Franzese A, Gargantini L, Greggio N, et al. 2008. The Italian National Survey for Prader–Willi syndrome: an epidemiologic study. *Am J Med Genet A* **146A:** 861–872. doi:10.1002/ajmg.a.32133

Gruhn JR, Zielinska AP, Shukla V, Blanshard R, Capalbo A, Cimadomo D, Nikiforov D, Chan AC, Newnham LJ, Vogel I, et al. 2019. Chromosome errors in human eggs shape natural fertility over reproductive life span. *Science* **365:** 1466–1469. doi:10.1126/science.aav7321

Hara-Isono K, Matsubara K, Fuke T, Yamazawa K, Satou K, Murakami N, Saitoh S, Nakabayashi K, Hata K, Ogata T, et al. 2020. Genome-wide methylation analysis in Silver–Russell syndrome, Temple syndrome, and Prader–Willi syndrome. *Clin Epigenetics* **12:** 159. doi:10.1186/s13148-020-00949-8

Haroske G, Baak JP, Danielsen H, Giroud F, Gschwendtner A, Oberholzer M, Reith A, Spieler P, Böcking A. 2001. Fourth updated ESACP consensus report on diagnostic DNA image cytometry. *Anal Cell Pathol* **23:** 89–95. doi:10.1155/2001/657642

Hoffmann K, Heller R. 2011. Uniparental disomies 7 and 14. *Best Pract Res Clin Endocrinol Metab* **25:** 77–100. doi:10.1016/j.beem.2010.09.004

Hoglund P, Holmberg C, de la Chapelle A, Kere J. 1994. Paternal isodisomy for Chromosome 7 is compatible with normal growth and development in a patient with congenital chloride diarrhea. *Am J Hum Genet* **55:** 747–752.

Inbar-Feigenberg M, Choufani S, Cytrynbaum C, Chen YA, Steele L, Shuman C, Ray PN, Weksberg R. 2013. Mosaicism for genome-wide paternal uniparental disomy with features of multiple imprinting disorders: diagnostic and management issues. *Am J Med Genet A* **161A:** 13–20. doi:10.1002/ajmg.a.35651

Joshi RS, Garg P, Zaitlen N, Lappalainen T, Watson CT, Azam N, Ho D, Li X, Antonarakis SE, Brunner HG, et al. 2016. DNA methylation profiling of uniparental disomy subjects provides a map of parental epigenetic bias in the human genome. *Am J Hum Genet* **99:** 555–566. doi:10.1016/j.ajhg.2016.06.032

Júlíusson PB, Roelants M, Eide GE, Moster D, Juul A, Hauspie R, Waaler PE, Bjerknes R. 2009. [Growth references for Norwegian children]. *Tidsskr Nor Laegeforen* **129:** 281–286. doi:10.4045/tidsskr.09.32473

Kalish JM, Conlin LK, Bhatti TR, Dubbs HA, Harris MC, Izumi K, Mostoufi-Moab S, Mulchandani S, Saitta S, States LJ, et al. 2013. Clinical features of three girls with mosaic genome-wide paternal uniparental isodisomy. *Am J Med Genet A* **161A:** 1929–1939. doi:10.1002/ajmg.a.36045

Kenny AP, Crimmins NA, Mackay DJ, Hopkin RJ, Bove KE, Leonis MA. 2009. Concurrent course of transient neonatal diabetes with cholestasis and paucity of interlobular bile ducts: a case report. *Pediatr Dev Pathol* **12:** 417–420. doi:10.2350/09-03-0628-CR.1

Kim D, Langmead B, Salzberg SL. 2015. HISAT: a fast spliced aligner with low memory requirements. *Nat Methods* **12:** 357–360. doi:10.1038/nmeth.3317

Kotzot D. 2008. Complex and segmental uniparental disomy updated. *J Med Genet* **45:** 545–556. doi:10.1136/jmg.2008.058016

Kotzot D, Utermann G. 2005. Uniparental disomy (UPD) other than 15: phenotypes and bibliography updated. *Am J Med Genet A* **136:** 287–305. doi:10.1002/ajmg.a.30483

Kotzot D, Holland H, Keller E, Froster UG. 2001. Maternal isochromosome 7q and paternal isochromosome 7p in a boy with growth retardation. *Am J Med Genet* **102:** 169–172. doi:10.1002/ajmg.1430

Le Caignec C, Isidor B, de Pontbriand U, David V, Audrezet MP, Ferec C, David A. 2007. Third case of paternal isodisomy for Chromosome 7 with cystic fibrosis: a new patient presenting with normal growth. *Am J Med Genet A* **143A:** 2696–2699. doi:10.1002/ajmg.a.31999

Lee CT, Tung YC, Hwu WL, Shih JC, Lin WH, Wu MZ, Kuo KT, Yang YL, Chen HL, Chen M, et al. 2019. Mosaic paternal haploidy in a patient with pancreatoblastoma and Beckwith–Wiedemann spectrum. *Am J Med Genet A* **179:** 1878–1883. doi:10.1002/ajmg.a.61276

Liao Y, Smyth GK, Shi W. 2014. featureCounts: an efficient general purpose program for assigning sequence reads to genomic features. *Bioinformatics* **30:** 923–930. doi:10.1093/bioinformatics/btt656

Liehr T. 2014. *Uniparental disomy (UPD) in clinical genetics.* Springer-Verlag, Berlin.

Love MI, Huber W, Anders S. 2014. Moderated estimation of fold change and dispersion for RNA-seq data with DESeq2. *Genome Biol* **15:** 550. doi:10.1186/s13059-014-0550-8

McCoy RC, Demko ZP, Ryan A, Banjevic M, Hill M, Sigurjonsson S, Rabinowitz M, Petrov DA. 2015. Evidence of selection against complex mitotic-origin aneuploidy during preimplantation development. *PLoS Genet* **11:** e1005601. doi:10.1371/journal.pgen.1005601

Naik S, Riordan-Eva E, Thomas NS, Poole R, Ashton M, Crolla JA, Temple IK. 2011. Large de novo deletion of 7p15.1 to 7p12.1 involving the imprinted gene GRB10 associated with a complex phenotype including

features of Beckwith–Wiedemann syndrome. *Eur J Med Genet* **54:** 89–93. doi:10.1016/j.ejmg.2010.09.006

Nakamura A, Muroya K, Ogata-Kawata H, Nakabayashi K, Matsubara K, Ogata T, Kurosawa K, Fukami M, Kagami M. 2018. A case of paternal uniparental isodisomy for Chromosome 7 associated with overgrowth. *J Med Genet* **55:** 567–570. doi:10.1136/jmedgenet-2017-104986

Nakka P, Pattillo Smith S, O'Donnell-Luria AH, McManus KF, 23andMe Research Team, Mountain JL, Ramachandran S, Sathirapongsasuti JF. 2019. Characterization of prevalence and health consequences of uniparental disomy in four million individuals from the general population. *Am J Hum Genet* **105:** 921–932. doi:10.1016/j.ajhg.2019.09.016

Ono R, Nakamura K, Inoue K, Naruse M, Usami T, Wakisaka-Saito N, Hino T, Suzuki-Migishima R, Ogonuki N, Miki H, et al. 2006. Deletion of *Peg10*, an imprinted gene acquired from a retrotransposon, causes early embryonic lethality. *Nat Genet* **38:** 101–106. doi:10.1038/ng1699

Ottolini CS, Newnham L, Capalbo A, Natesan SA, Joshi HA, Cimadomo D, Griffin DK, Sage K, Summers MC, Thornhill AR, et al. 2015. Genome-wide maps of recombination and chromosome segregation in human oocytes and embryos show selection for maternal recombination rates. *Nat Genet* **47:** 727–735. doi:10.1038/ng.3306

Pan Y, McCaskill CD, Thompson KH, Hicks J, Casey B, Shaffer LG, Craigen WJ. 1998. Paternal isodisomy of Chromosome 7 associated with complete situs inversus and immotile cilia. *Am J Hum Genet* **62:** 1551–1555. doi:10.1086/301857

Patten MM, Cowley M, Oakey RJ, Feil R. 2016. Regulatory links between imprinted genes: evolutionary predictions and consequences. *Proc Biol Sci* **283:** 20152760. doi:10.1098/rspb.2015.2760

Pertea M, Kim D, Pertea GM, Leek JT, Salzberg SL. 2016. Transcript-level expression analysis of RNA-seq experiments with HISAT, StringTie and Ballgown. *Nat Protoc* **11:** 1650–1667. doi:10.1038/nprot.2016.095

Postema FAM, Bliek J, van Noesel CJM, van Zutven L, Oosterwijk JC, Hopman SMJ, Merks JHM, Hennekam RC. 2019. Multiple tumors due to mosaic genome-wide paternal uniparental disomy. *Pediatr Blood Cancer* **66:** e27715. doi:10.1002/pbc.27715

Sanchez-Delgado M, Martin-Trujillo A, Tayama C, Vidal E, Esteller M, Iglesias-Platas I, Deo N, Barney O, Maclean K, Hata K, et al. 2015. Absence of maternal methylation in biparental hydatidiform moles from women with *NLRP7* maternal-effect mutations reveals widespread placenta-specific imprinting. *PLoS Genet* **11:** e1005644. doi:10.1371/journal.pgen.1005644

Scuffins J, Keller-Ramey J, Dyer L, Douglas G, Torene R, Gainullin V, Juusola J, Meck J, Retterer K. 2021. Uniparental disomy in a population of 32,067 clinical exome trios. *Genet Med* **23:** 1101–1107. doi:10.1038/s41436-020-01092-8

Sheppard SE, Lalonde E, Adzick NS, Beck AE, Bhatti T, De Leon DD, Duffy KA, Ganguly A, Hathaway E, Ji J, et al. 2019. Androgenetic chimerism as an etiology for Beckwith–Wiedemann syndrome: diagnosis and management. *Genet Med* **21:** 2644–2649. doi:10.1038/s41436-019-0551-9

Subramanian A, Tamayo P, Mootha VK, Mukherjee S, Ebert BL, Gillette MA, Paulovich A, Pomeroy SL, Golub TR, Lander ES, et al. 2005. Gene set enrichment analysis: a knowledge-based approach for interpreting genome-wide expression profiles. *Proc Natl Acad Sci* **102:** 15545–15550. doi:10.1073/pnas.0506580102

Tyc KM, McCoy RC, Schindler K, Xing J. 2020. Mathematical modeling of human oocyte aneuploidy. *Proc Natl Acad Sci* **117:** 10455–10464. doi:10.1073/pnas.1912853117

Watanabe K, Taskesen E, van Bochoven A, Posthuma D. 2017. Functional mapping and annotation of genetic associations with FUMA. *Nat Commun* **8:** 1826. doi:10.1038/s41467-017-01261-5

Xie T, Pan S, Zheng H, Luo Z, Tembo KM, Jamal M, Yu Z, Yu Y, Xia J, Yin Q, et al. 2018. PEG10 as an oncogene: expression regulatory mechanisms and role in tumor progression. *Cancer Cell Int* **18:** 112. doi:10.1186/s12935-018-0610-3

Xu J, Zhang M, Niu W, Yao G, Sun B, Bao X, Wang L, Du L, Sun Y. 2015. Genome-wide uniparental disomy screen in human discarded morphologically abnormal embryos. *Sci Rep* **5:** 12302. doi:10.1038/srep12302